analytical chemistry

Article

pubs.acs.org/ac

Chemiluminescence Imaging Immunoassay of Multiple Tumor Markers for Cancer Screening

Chen Zong,[†] Jie Wu,[†] Chen Wang,[†] Huangxian Ju,*[,†] and Feng Yan*[,‡]

[†]State Key Laboratory of Analytical Chemistry for Life Science, Department of Chemistry, Nanjing University, Nanjing 210093, People's Republic of China

[‡]Jiangsu Institute of Cancer Prevention and Cure, Nanjing 210009, People's Republic of China

Supporting Information

ABSTRACT: A sensitive chemiluminescence (CL) imaging immunoassay method for detection of multiple tumor markers with high throughput, easy operation, and low cost was developed. The immunosensor array was prepared by covalently immobilizing capture antibodies on corresponding sensing sites on a silanized disposable glass chip. Gold nanoparticle-based bioconjugates with a high molar ratio of horseradish peroxidase (HRP) to detection antibodies were used for signal amplification. Under a sandwich immunoassay, the CL signals triggered by HRP captured on each sensing cell were collected by a charge-coupled device for simultaneous measurement of biomarkers and combination diagnosis of certain tumors. As a proof of concept, the immunosensor array was applied to detect α-fetoprotein, carcinoma antigen 125, carbohydrate antigen 153, and carcinoembryonic antigen and to screen patients with liver, breast, or ovarian cancers. This method showed wide linear ranges over 5 orders of magnitude and much lower detection limits than previously reported multiplexed immunoassays. The high throughput and acceptable stability, reproducibility, and accuracy showed good applicability of the proposed multiplex CL imaging immunoassay in clinical diagnosis.

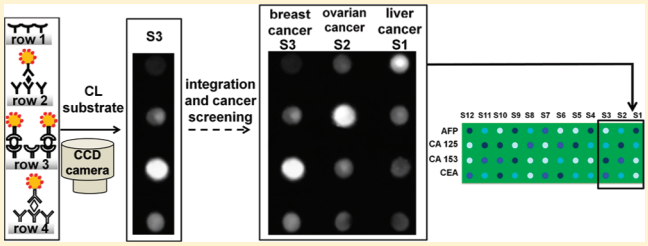

Early diagnosis and treatment of cancer are the keys to improve patient survival rate. As the levels of tumor markers in serum are associated with the stages of tumors, reliable and sensitive determination of tumor markers plays a significant role in early cancer screening and evaluation.[1−3] Recently, great efforts have been made to develop novel immunoassay methods and immunosensors combined with diverse detection strategies, such as electrochemical, optical, and mass techniques, for the detection of protein markers.[3−6] Among these detection methods, owing to the limited specificity of single markers in cancer diagnosis, multiplex immunoassays for analyzing a panel of tumor markers in complex serum samples to improve the diagnostic accuracy have attracted considerable attention.[7,8] In comparison with parallel single-analyte methods, multiplex assays can enhance sample throughput, shorten assay time, and decrease sample consumption and cost.[9,10]

Generally, multianalyte assays can be performed in two dominant modes, spatial-resolved[11−14] and multilabel modes.[15] Multilabel mode needs to simultaneously detect various signals from different labels and, hence, often suffers difficulty in accurate quantification because of the signal overlap and different optimal assay conditions of these labels.[16] To overcome these drawbacks, several multilabel resolution strategies have been reported.[17,18] However, it remains difficult to achieve the simultaneous detection of a large number of protein markers due to the restriction in the number of available labels.

Spatial-resolved mode with a single label can simultaneously detect different targets in different immunoreaction areas on one substrate. Various spatial-resolved arrays, such as electrochemical[19−21] and optical[22,23] sensor arrays, have been emerged in the past decade. For example, Kwon et al.[24] fabricated a 25 × 8 protein array with fluorescence detection for rapid determination of blood coagulation factor XIII activity, and Wilson and Nie[2] reported a series of electrochemical sensor arrays for simultaneous quantitative detection of seven tumor markers. Our previous works fabricated various disposable electrochemical chips for multiplex immunoassay of two or four tumor markers.[13,25] Besides the fluorescence and electrochemical arrays, a chemiluminescence (CL)-based array coupled with a charge-coupled device (CCD) as detector has attracted considerable interest.[26] A polystyrene 96 × 4 well microtiter plate has been designed for CL screening of four pathogenic bacteria in foodstuffs.[27] A multichannel flow-through CL microarray chip has also been proposed for parallel detection of three bacteria.[28] Although CL detection can be used for simple design of sensor setup because there is no need of external light source or optics, the sensitivity of CL assays is relatively low, which makes this detection technique difficult to apply in the detection of low-abundance biomarkers in cancer screening.

Received: November 30, 2011
Accepted: February 8, 2012
Published: February 8, 2012

Scheme 1. Schematic Diagrams of Immunosensors Array with 4 × 12 Cells and CL Imaging Immunoassay Procedure[a]

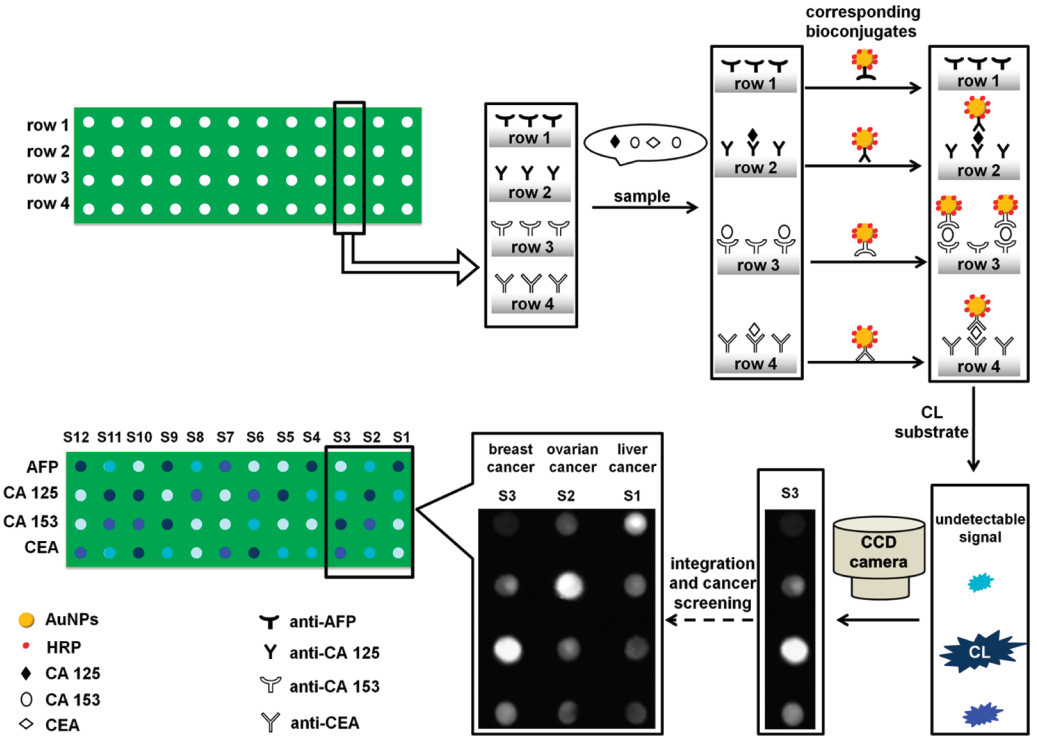

[a]Anti-AFP, CA 125, CA 153, and CEA antibodies (Ab1) were immobilized on rows 1−4, respectively. Each column was used to simultaneously detect four targets in a single sample. S1−S12 represent 12 samples. The sample solution was distributed into four cells in the same column for sandwich immunoassay. After incubation with the sample and then the tag, the CL substrates were dropped in the cells to collect the CL image by CCD. The sample shown was distributed in column 3, which shows a high level of CA 153 (row 3), middle levels of CA 125 and CEA (rows 2 and 4), and undetectable AFP (row 1).

Recently, catalytic nanomaterials[29] and carbon nanotubes[30] have been used in the fabrication of CL sensor arrays to improve sensitivity. Signal amplification strategies have been adopted to combine with CL immunoassay for the development of sensitive CL-based immunoassays. Bioconjugation of large amounts of signal molecules to a single protein such as secondary antibody by a carrier has become an attractive signal amplification approach. Gold nanoparticles (AuNPs) are widely used carriers of signal molecules.[31−34] In this work, four tags were prepared by binding a high loading ratio of horseradish peroxidase (HRP) to detection antibodies (Ab2) to AuNPs. By combining the AuNP-based tags with a CL sensor array and a sensitive cooled low-light CCD, a highly sensitive CL imaging immunoassay method was proposed for simultaneous detection of biomarkers. The immunosensor array was fabricated on a glass slide by a convenient screen-printing technique. The disposable array including 48 sensing cells (4 rows ×12 columns) could simultaneously detect four tumor markers in 12 samples, which provides a promising application in high-throughput cancer screening.

EXPERIMENTAL SECTION

Materials and Reagents. The capture antibodies (Ab1) and Ab2 of α-fetoprotein (AFP) (mouse monoclonal antibodies, clones bsm-1021 and bsm-1022), carcinoembryonic antigen (CEA) (mouse monoclonal antibodies, clones bsm-1023 and bsm-1024), carcinoma antigen 125 (CA 125) (rabbit polyclonal antibodies, clone bs-0091R), and carbohydrate antigen 153 (CA 153) (rabbit polyclonal antibodies, clone bs-1239R), as well as HRP, were purchased from Beijing Biosynthesis Biotechnology Co. Ltd. (Beijing, China). Commercial CL enzyme-linked immunosorbent assay (ELISA) kits, including standard solutions with concentrations from 10 to 500 ng/mL (AFP), 15−400 units/mL (CA 125), 15−240 units/mL (CA 153), and 5−160 ng/mL (CEA), and CL substrate solutions for HRP (luminol-*p*-iodophenol and H_2O_2), were obtained from Autobio Diagnostics Co., Ltd. (China). The corresponding electrochemiluminescent (ECL) immunoassay reagent kits for reference detection were provided by Roche Diagnostics GmbH (Germany). Chloroauric acid ($HAuCl_4{\cdot}4H_2O$) and trisodium citrate were obtained from Shanghai Reagent Co. (Shanghai, China). 3-Glycidoxypropyltrimethoxysilane (GPTMS) and bovine serum albumin (BSA) were purchased from Sigma−Aldrich Chemical Co. (St. Louis, MO). Tween-20 was obtained from Sinopharm Chemical Reagent Co. Ltd. (China). Phosphate-buffered saline (PBS; 0.01 M, pH 7.4), prepared by mixing the stock solutions of NaH_2PO_4 and Na_2HPO_4, was used as coupling buffer for the immobilization of Ab1. Washing buffer was 0.01 M PBS spiked with 0.05% Tween-20 (pH 7.4). Blocking buffer, which was used to block the residual reactive sites on the antibody-immobilized arrays, was 0.01 M PBS containing 5% BSA (pH 7.4). Ultrapure water obtained from a Millipore water purification system (≥18 MΩ, Milli-Q, Millipore) was used in all assays. Clinical serum samples were from Jiangsu Cancer Hospital. All other reagents were of analytical grade and used as received.

Apparatus. A cooled low-light CCD camera with high resolution (BioImaging Systems Chemi HR 410 camera, UVP) was used to collect the CL signals in all measurements. Kinetic behavior of the CL reaction catalyzed by HRP label on the

dx.doi.org/10.1021/ac203179g | *Anal. Chem.* 2012, 84, 2410−2415

sandwich immunocomplex was studied with a static method on an IFFM-E luminescent analyzer (Remax, China). The ultraviolet−visible (UV−vis) spectroscopic experiment was performed with a UV-3600 UV−vis spectrophotometer (Shimadzu, Japan) to demonstrate the preparation of Ab2−AuNP−HRP bioconjugates. Scanning electron micrographs were obtained with a Hitachi S-3000N scanning electron microscope (Japan) at an acceleration voltage of 10 kV. The control levels of the tumor markers in sera were obtained with an automated ECL analyzer (Elecsys 2010; Roche).

Fabrication of Immunosensor Array. The immunosensor array contained 48 sensing cells (2 mm diameter) in a 4 rows × 12 columns format (Scheme 1). The antibodies to AFP, CA 125, CA 153, and CEA were immobilized on different rows. Each column could be used to simultaneously detect four targets in a single sample; thus 12 columns could be simultaneously used to detect 12 samples.

First, a microscope glass slide was activated with piranha solution (H_2SO_4/30% H_2O_2, 7:3 in volume) for 12 h to bring hydroxyl group on its surface. After being washed with water and dried by nitrogen, the activated glass slide was silanized with 1% GPTMS/toluene solution overnight at room temperature (25 °C). Then, sequential washes with toluene and ethanol were used to remove the physically absorbed silane from the surface, followed by drying with nitrogen. Finally, a layer of hydrophobic photoinactive film with 48 cells (2 mm diameter, 4 mm edge-to-edge separation) in a 4 × 12 format was printed on the treated microscope slide by screen-printing technology, which was completed by use of a film template with 48 plots. These formed cells could be used as reservoirs to align the antibody and other solutions for immunoassay.

Capture antibodies (1.5 μL) for AFP, CA 125, CA 153, and CEA at 10 μg/mL were individually dropped on silanized sites exposed in four rows, respectively, and incubated overnight at 4 °C. After the slides were washed with washing buffer and dried by nitrogen, 1.5 μL of blocking buffer was coated on each sensing site for 1 h to block the unreacted epoxy group. Finally, the immunosensor array was washed with washing buffer and stored in PBS at 4 °C before use. All washing steps were manually carried out with a washing bottle.

Preparation of Ab2−AuNP−HRP Bioconjugates. AuNPs were synthesized according to the previous protocol.[32] Briefly, an aqueous solution of 0.01% $HAuCl_4$ (100 mL) was boiled with vigorous stirring, and 3.5 mL of 1% trisodium citrate solution was added quickly, dropwise, to the boiling solution. The color of the solution turned from gray yellow to deep red, indicating the formation of AuNPs. The solution was kept stirring and was cooled down to room temperature.

Ab2−AuNP−HRP bioconjugates were prepared in accordance with the literature[33] with minor modification. Briefly, 10 μL of 100 μg/mL Ab2 and 24 μL of 5.0 mg/mL HRP were added into 1.0 mL of AuNP solution adjusted to pH 9.0. The solution was gently mixed for 2 h to form the Ab2−AuNP−HRP bioconjugates. Excess Ab2 and HRP were removed by centrifugation at 10 000 rpm for 30 min at 4 °C, and the precipitate was redispersed in 0.01 M PBS. This procedure was repeated two times. Finally, the obtained Ab2−AuNP−HRP bioconjugates were resuspended in 1.0 mL of 0.01 M PBS containing 1% BSA and stored at 4 °C.

Chemiluminescence Imaging Immunoassay. The CL imaging immunoassay for simultaneous multianalyte detection is illustrated in Scheme 1. To obtain the calibration curves of AFP, CA 125, CA 153, and CEA, 1.5 μL aliquots of the standard solutions diluted with 0.01 M PBS, pH 7.4, to different concentrations were added to the sensing sites on corresponding detection rows and incubated for 15 min. After the slides were rinsed with washing buffer and dried, 1.5 μL aliquots of Ab2−AuNP−HRP bioconjugates were added to corresponding sensing sites for 20 min, followed by washing and drying. Finally, 1.5 μL aliquots of a mixture of CL substrates were delivered into the sensing cells to trigger the CL reaction. To perform cancer screening, 1.5 μL of serum sample was added to four sensing cells in one column to perform the same procedures.

The CL signals were simultaneously collected by CCD with five 2-min exposure times for dynamic integration of 10 min. Spots were automatically identified by use of VisionWorksLS image acquisition and analysis software (UVP). The CL intensity of each spot was calculated as the mean pixel intensity within a square of a given side length around each spot center.

RESULTS AND DISCUSSION

Characterization of Immunosensor Array. Epoxy group was used to activate the glass slide for binding Ab1 on the sensing cells. After treatment with piranha solution, the glass slide showed a smooth and homogeneous surface (Supporting Information, Figure S1a). Upon immobilization of Ab1, an obvious aggregation of the trapped biomolecules with a regular distribution on the surface could be observed (Supporting Information, Figure S1b,c), indicating successful assembly of Ab1 on the sensing sites.

Characterization of Ab2−AuNP−HRP Bioconjugates. UV−vis spectra were used to characterize the formation of Ab2−AuNP−HRP bioconjugates. Compared with AuNPs (Supporting Information, Figure S2, curve a), the UV−vis spectrum of Ab2−AuNP−HRP bioconjugates showed a wider absorption peak with a red shift from 519.0 to 523.0 nm (Supporting Information, Figure S2, curve b), indicating that a slight aggregation of the nanoparticles occurred after the binding of Ab2 and HRP onto AuNPs. Moreover, the Ab2−AuNP−HRP bioconjugate solution showed a 278.5 nm absorption peak corresponding to the typical protein absorption, indicating the existence of protein on the surface of AuNPs.

Signal Amplification by Ab2−AuNP−HRP Tracing Tag. In order to evaluate the amplification ability of Ab2−AuNP−HRP tag, sandwich immunoassays with both Ab2−AuNP−HRP and Ab2−HRP labels were performed on the proposed CL sensing array with the same detection conditions. As shown in Figure 1, the Ab2−AuNP−HRP bioconjugates produced an 8-fold higher signal (intensity 2074) than that of Ab2−HRP (intensity 251), along with similar noise (intensity 59 versus 56), hence leading to an 8-fold higher signal-to-noise ratio (S/N).

The nonspecific binding character of the Ab2−AuNP−HRP tag was also evaluated by use of the CEA assay as a model. Chemiluminescent intensity on the CEA sensing cell incubated with 0.1 ng/mL CEA and anti-AFP−AuNP−HRP was 76 (Supporting Information, Figure S3), which was close to the noise of 59 detected in the absence of CEA, indicating that little nonspecific binding occurred between antigen and nonspecific tags. When the albumin-passivated off-well sites were incubated with Ab2−AuNP−HRP tag, the cell showed a CL intensity of 53 (Supporting Information, Figure S3); thus the nonspecific adsorption of Ab2−AuNP−HRP tag was negligible.

dx.doi.org/10.1021/ac203179g | Anal. Chem. 2012, 84, 2410−2415

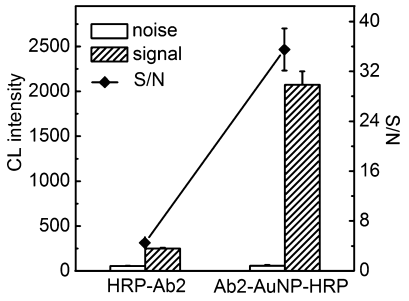

Figure 1. Performance of Ab2−AuNP−HRP tag compared with Ab2−HRP label on the sensing array with the same detection conditions. Signal and noise are the CL intensities obtained from the immunoassays in the presence and absence of 0.1 ng/mL CEA. Results are expressed as the average of three independent experiments. Error bars represent standard deviations (SD).

Kinetic Characteristics of the Chemiluminescence Reaction. Kinetic behavior of the CL reaction catalyzed by Ab2−AuNP−HRP tracing tag labeled to the sandwich immunocomplex was studied with a static method. The CL reaction occurred immediately upon the addition of CL substrates. The intensity of the CL emission increased quickly to the maximum value and then decreased slowly (Supporting Information, Figure S4), indicating higher sensitivity could be obtained in a short measurement time (about 1 min). However, CCD imaging demanded a long exposure time to collect the weak CL signal for realizing highly sensitive immunoassay. In this work, as the CL intensity could be retained at 80% of the maximum value after CL reaction for 10 min, an exposure time of 10 min was used for dynamic integration to collect the CL signal.

Incubation Times. The performance of CL imaging immunoassay depended on the formation of sandwich immunocomplex, which was related to the incubation temperature and times. For convenient manipulation, the incubation steps were performed at room temperature (25 °C). The effect of incubation times was examined by use of 1.0 ng/mL AFP and CEA, and 1.0 unit/mL CA 125 and CA 153. The CL responses to four tumor markers increased with increasing incubation times with antigens (Supporting Information, Figure S5) and Ab2−AuNP−HRP bioconjugates (Supporting Information, Figure S6), and all trended to their maximum values at 15 and 20 min, respectively, indicating the saturated binding of antigen to Ab1 and Ab2−AuNP−HRP bioconjugates to Ab1−antigen complex on the sensing sites. Thus, incubation times of 15 and 20 min were chosen for the two incubation steps in the sandwich immunoassay.

Assay Performance. The analytical performance of the CL imaging immunoassay was characterized under optimal experimental conditions. After two-step incubation and triggering the CL reaction, the sensing sites showed bright spots (Figure 2a). The brightness corresponded to the concentration of analyte. The collected CL intensity was proportional to the logarithm of analyte concentration over the ranges of (5.0×10^{-5})−10 ng/mL for AFP, (1.0×10^{-4})−20 units/mL for CA 125, (1.0×10^{-4})−10 units/mL for CA 153, and (5.0×10^{-5})−10 ng/mL for CEA (Figure 2b). The detection limits corresponding to the signals of 3 SD for these tumor markers were 7×10^{-6} ng/mL, 1.7×10^{-5} unit/mL, 8.6×10^{-6} unit/mL, and 1.6×10^{-5} ng/mL, respectively, which were much lower than those reported previously in multiplexed immunoassays,[2,13,17,18,35,36] and also 220−530 times lower than

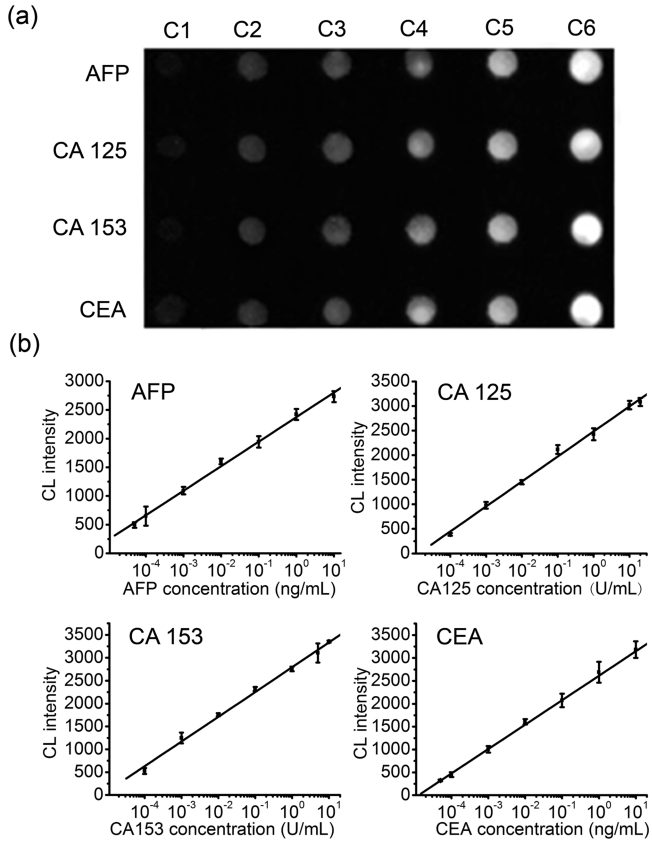

Figure 2. (a) CL image and (b) calibration curves for immunoassay of tumor markers. C1−C6 represent concentrations of 10^{-4}, 10^{-3}, 10^{-2}, 10^{-1}, 1, and 10: ng/mL for AFP and CEA and units/mL for CA 125 and CA 153.

the values for Ab2−HRP label of 3.7×10^{-3} ng/mL, 4.1×10^{-3} unit/mL, 4.2×10^{-3} unit/mL, and 3.6×10^{-3} ng/mL, respectively. Low limits of detection (LOD) and high sensitivity could improve the detection precision and detect the concentrations of proteins at low levels in serum. The assay showed potential application in tracking tumor recurrence and progression in a minimal residual disease context.

The immunosensor array could be stored in PBS at 4 °C. After a storage period of 30 days, the CL responses of the AFP, CA 125, CA 153, and CEA immunosensors were 89.8%, 94.5%, 89.7%, and 90.7% of their initial responses, respectively, indicating acceptable stability.

Sample Throughput. High sample throughput is a long-cherished goal in the developments of both immunosensors and multianalyte testing. It is of great significance in early disease screening. To achieve this goal, short analytical time per assay is necessary. The proposed CL imaging immunoassay method possessed this advantage. The total testing process on one array could be completed within 48 min, including a total incubation time of 35 min for two-step sandwich immunoreaction, an exposure time of 10 min for the CCD-based signal collection, and washing. This means the simultaneous detection of 48 samples could be carried out in 48 min, leading to a throughput of 60 testing per hour for single analyte measurement and 15 samples per hour for cancer screening by a panel of four tumor markers. The throughput greatly depended on the number of sensing cells per chip. For example, the CCD camera used in this assay could offer a screen window of 90 mm × 70 mm for 180 sensing cells with 2-mm diameter

dx.doi.org/10.1021/ac203179g | Anal. Chem. 2012, 84, 2410−2415

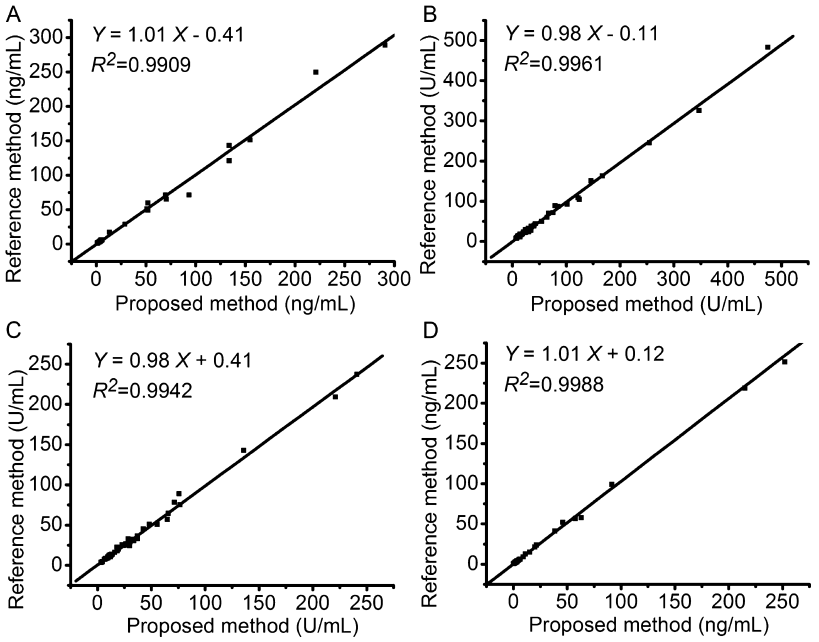

Figure 3. Samples (n = 60) assayed for correlation studies. Results of simultaneous multianalyte immunoassay of (A) AFP, (B) CA 125, (C) CA 153, and (D) CEA in human sera were compared with reference single-analyte immunoassays.

and 4-mm side-to-side distance. Furthermore, parallel incubation could be conveniently performed on several chips, and the CL imaging detection needed only 10 min, which led to a higher throughput when more chips were used for parallel incubation and immunoassay.

Detection of Tumor Markers in Clinical Serum Samples. To evaluate the analytical reliability and application potential of the proposed CL imaging immunoassay, 60 clinical serum samples were tested as compared to commercial ECL single-analyte testing. When the levels of tumor markers were higher than the upper limit of calibration ranges, serum samples were serially diluted 10, 100, 1000, and 10 000 times with 0.01 M PBS, pH 7.4, prior to the assay. As shown in Figure 3, both the good correlation coefficients (R^2 > 0.99) and the slopes close to 1 indicated acceptable accuracy of the proposed assay.

Cancer Screening. According to the panel of tumor markers for combination diagnosis of certain tumors (AFP–CEA panel for liver cancer, CA 125–CEA–AFP panel for ovarian cancer, and CA 153–CA 125–CEA panel for breast cancer),[3] the proposed CL imaging immunoassay method was used to screen liver, breast, and ovarian cancers. As AFP, CA 153, and CA 125 are the most cancer-specific markers for liver, breast, and ovarian cancers, respectively, their levels in serum samples from patients with these cancers are much higher than their clinical thresholds. Hence, the CL image of the sensing cells for these markers showed the highest brightness in the marker panel corresponding to liver, breast, and ovarian cancers, respectively (Figure 4). CEA is a popular tumor marker and shows higher level than its clinical threshold in many tumors; thus it was used to confirm the presence of other cancers in this work.

Positive detection rates in 102 serum samples by the CL imaging immunoassay are shown in Table 1. The positive detection rates of AFP–CEA panel for 20 cases of liver cancer and CEA for 15 cases of other cancers were 100%, while CA 153–CA 125–CEA panel for 28 cases of breast cancer and CA 125–CEA–AFP panel for 32 cases of ovarian cancer showed positive detection rates of 96.4% and 96.9%, respectively. As

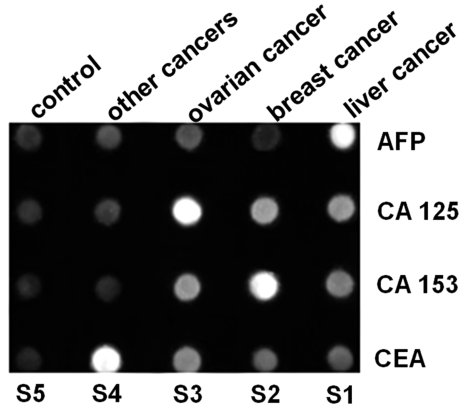

Figure 4. Cancer screening for five serum samples. S1, S2, S3, and S4 represent serum samples from patients with liver, breast, ovarian, and other cancers. S5 represents the normal control.

controls, no positive results were obtained in seven normal control samples. These results demonstrated the improved positive detection rates and diagnostic value for cancer screening, showing potential application in clinic diagnosis.

CONCLUSIONS

This work reports a novel chemiluminescence imaging immunoassay of multiple tumor markers with high throughput, low cost, small consumption, simple operation, and high sensitivity for combination diagnosis of certain tumors. The use of AuNP-based multienzymatic amplification leads to a wide linear detection range and much lower detection limits for biomarkers as compared to the assay with single enzyme tags. With the introduction of spot array enterprise system, the proposed method is easy to adapt for automation and further simplification. The immunosensor array has acceptable stability, reproducibility, and accuracy. The availability of this system to measure simultaneously the levels of multimarkers in serum samples with excellent sensitivity, throughput, and accuracy is

dx.doi.org/10.1021/ac203179g | Anal. Chem. 2012, 84, 2410–2415

Table 1. Positive Detection Rates of Clinical Sera

sample	*n*	associated tumor markers	positive cases (*n*)	positive detection rate (%)
liver cancer	20	AFP,[a] CEA	20[b]	100
breast cancer	28	CA 153,[a] CA 125, CEA	27[b]	96.4
ovarian cancer	32	CA 125,[a] AFP, CEA	31[b]	96.9
other cancers	15	CEA	15[b]	100
control	7	AFP, CA 125, CA 153, CEA	0[c]	0

[a]The level of relatively specific marker to certain tumor, for example, AFP to liver cancer, CA 125 to ovarian cancer, and CA 153 to breast cancer, has the biggest difference from its cutoff value. [b]All concentrations of the associated tumor markers obtained with the proposed method are higher than the clinical cutoff values of individual tumor markers (AFP, 6 ng/mL; CA 125, 35 units/mL; CA 153, 25 units/mL; CEA, 3 ng/mL), while the levels of other markers are normally under the cutoff values. [c]Cases with concentrations of ≥1 tumor markers are higher than their clinical cutoff values.

suitable to carry out large-scale screening of cancers in the early stage.

■ ASSOCIATED CONTENT

Ⓢ Supporting Information

Six figures and one table as described in the text. This material is available free of charge via the Internet at http://pubs.acs.org.

■ AUTHOR INFORMATION

Corresponding Author

*(H.J.) phone/fax +86-25-83593593, e-mail hxju@nju.edu.cn; (F.Y.) e-mail yanfeng2007@sohu.com.

Notes

The authors declare no competing financial interest.

■ ACKNOWLEDGMENTS

This work was financially supported by National Basic Research Program (2010CB732400), National Natural Science Foundation of China (21075055, 21135002, 21121091), and the Leading Medical Talents Program from Department of Health of Jiangsu Province.

■ REFERENCES

(1) Lin, J. H.; Ju, H. X. *Biosens. Bioelectron.* **2005**, *20*, 1461−1470.
(2) Wilson, M. S.; Nie, W. Y. *Anal. Chem.* **2006**, *78*, 6476−6483.
(3) Wu, J.; Fu, Z. F.; Yan, F.; Ju, H. X. *TrAC, Trends Anal. Chem.* **2007**, *26*, 679−688.
(4) Soper, S. A.; Brown, K.; Ellington, A.; Frazier, B.; Garcia-Manero, G.; Gau, V.; Gutman, S. I.; Hayes, D. F.; Korte, B.; Landers, J. L.; Larson, D.; Ligler, F.; Majumdar, A.; Mascini, M.; Nolte, D.; Rosenzweig, Z.; Wang, J.; Wilson, D. *Biosens. Bioelectron.* **2006**, *21*, 1932−1942.
(5) Rasooly, A.; Jacobson, J. *Biosens. Bioelectron.* **2006**, *21*, 1851−1858.
(6) Wang, J. *Biosens. Bioelectron.* **2006**, *21*, 1887−1892.
(7) Sanchez-Carbayo, M. *Clin. Chem.* **2006**, *52*, 1651−1659.
(8) Zheng, G. F.; Patolsky, F.; Cui, Y.; Wang, W. U.; Lieber, C. M. *Nat. Biotechnol.* **2005**, *23*, 1294−1301.
(9) Kricka, L. J. *Clin. Chem.* **1992**, *38*, 327−328.
(10) Zhang, S. C.; Zhang, C.; Xing, Z. *Clin. Chem.* **2004**, *50*, 1214−1221.
(11) Rowe, C. A.; Scruggs, S. B.; Feldstein, M. J.; Golden, J. P.; Ligler, F. S. *Anal. Chem.* **1999**, *71*, 433−439.
(12) Knecht, B. G.; Strasser, A.; Dietrich, R.; Märtlbauer, E.; Niessner, R.; Weller, M. G. *Anal. Chem.* **2004**, *76*, 646−654.
(13) Wu, J.; Yan, F.; Tang, J. H.; Zhai, C.; Ju, H. X. *Clin. Chem.* **2007**, *53*, 1495−1502.
(14) Wu, J.; Yan, F.; Zhang, X. Q.; Yan, Y. T.; Tang, J. H.; Ju, H. X. *Clin. Chem.* **2008**, *54*, 1481−1488.
(15) Li, H.; Gao, Z. J.; Zhang, Y. H.; Lau, C.; Lu, J. Z. *Anal. Methods* **2010**, *2*, 1236−1242.
(16) Goldman, E. R.; Clapp, A. R.; Anderson, G. P.; Uyeda, T.; Mauro, J. M.; Medintz, I. L.; Mattoussi, H. *Anal. Chem.* **2004**, *76*, 684−688.
(17) Fu, Z. F.; Liu, H.; Ju, H. X. *Anal. Chem.* **2006**, *78*, 6999−7005.
(18) Fu, Z. F.; Yang, Z. J.; Tang, J. H.; Liu, H.; Yan, F.; Ju, H. X. *Anal. Chem.* **2007**, *79*, 7376−7382.
(19) Wilson, M. S.; Nie, W. Y. *Anal. Chem.* **2006**, *78*, 2507−2513.
(20) Wilson, M. S. *Anal. Chem.* **2005**, *77*, 1496−1502.
(21) Kojima, K.; Hiratsuka, A.; Suzuki, H.; Yano, K.; Ikebukuro, K.; Karube, I. *Anal. Chem.* **2003**, *75*, 1116−1122.
(22) Jiang, X. Y.; Ng, J. M. K.; Stroock, A. D.; Dertinger, S. K. W.; Whitesides, G. M. *J. Am. Chem. Soc.* **2003**, *125*, 5294−5295.
(23) Delehanty, J. B.; Ligler, F. S. *Anal. Chem.* **2002**, *74*, 5681−5687.
(24) Kwon, M. H.; Kong, D. H.; Jung, S. H.; Suh, I. B.; Kim, Y. M.; Ha, K. S. *Anal. Chem.* **2011**, *83*, 2317−2323.
(25) Wu, J.; Zhang, Z. J.; Fu, Z. F.; Ju, H. X. *Biosens. Bioelectron.* **2007**, *23*, 114−120.
(26) Stephen, P. F.; John, V. L.; Robert, I. M.; EI, O. B. *Clin. Chem.* **2005**, *51*, 1165−1176.
(27) Magliulo, M.; Simoni, P.; Guardigli, M.; Michelini, E.; Luciani, M.; Lelli, R.; Roda, A. *J. Agric. Food Chem.* **2007**, *55*, 4933−4939.
(28) Xaver, Y. Z. K.; Reinhard, N.; Michael, S. *Anal. Bioanal. Chem.* **2009**, *395*, 1623−1630.
(29) Kong, H.; Liu, D.; Zhang, S. C.; Zhang, X. R. *Anal. Chem.* **2011**, *83*, 1867−1870.
(30) Yang, M. H.; Kostov, Y.; Bruck, H. A.; Rasooly, A. *Anal. Chem.* **2008**, *80*, 8532−8537.
(31) Zhen, L.; Sauceda-Friebe, J. C.; Lin, J. M.; Niessner, R.; Knopp, D. *Anal. Methods* **2010**, *2*, 824−830.
(32) Ambrosi, A.; Castañeda, M. T.; Killard, A. J.; Smyth, M. R.; Alegret, S.; Merkoci, A. *Anal. Chem.* **2007**, *79*, 5232−5240.
(33) Cui, R. J.; Huang, H. P.; Yin, Z. Z.; Gao, D.; Zhu, J. J. *Biosens. Bioelectron.* **2008**, *23*, 1666−1673.
(34) Bi, S.; Yan, Y. M.; Yang, X. Y.; Zhang, S. S. *Chem.—Eur. J.* **2009**, *15*, 4704−4709.
(35) Yang, Z. J.; Liu, H.; Zong, C.; Yan, F.; Ju, H. X. *Anal. Chem.* **2009**, *81*, 5484−5489.
(36) Lai, G. S.; Yan, F.; Ju, H. X. *Anal. Chem.* **2009**, *81*, 9730−9736.